Electrochemical CO_2 reduction on a copper foam electrode at elevated pressures

Girichandran, Nandalal; Saedy, Saeed; Kortlever, Ruud

DOI
10.1016/j.cej.2024.150478

Publication date
2024

Document Version
Final published version

Published in
Chemical Engineering Journal

Chemical Engineering Journal 487 (2024) 150478

Contents lists available at ScienceDirect

Chemical Engineering Journal

journal homepage: www.elsevier.com/locate/cej

Electrochemical CO_2 reduction on a copper foam electrode at elevated pressures

Nandalal Girichandran [a], Saeed Saedy [b], Ruud Kortlever [a,*]

[a] Process & Energy Department, Faculty of Mechanical, Maritime and Materials Engineering, Large-Scale Energy Storage, Delft University of Technology, Leeghwaterstraat 39 2628 CB, Delft, the Netherlands
[b] Department of Chemical Engineering, Delft University of Technology, Van der Maasweg 9, Delft 2629 HZ, the Netherlands

A B S T R A C T

Electrochemical CO_2 reduction is a promising way of closing the carbon cycle while synthesizing useful commodity chemicals and fuels. One of the possible routes to scale up the process is CO_2 reduction at elevated pressure, as this is a way to increase the concentration of poorly soluble CO_2 in aqueous systems. Yet, not many studies focus on this route, owing to the inherent challenges with high-pressure systems, such as leaks, product quantification, and ease of operation. In this study, we use a high-pressure flow cell setup to investigate the impact of CO_2 pressure on the electrochemical performance of a copper foam electrode for CO_2 reduction within a pressure range of 1 to 25 bar. Our initial findings using a 0.5 M potassium bicarbonate ($KHCO_3$) electrolyte show a consistent improvement in selectivity towards CO_2 reduction products, with HCOOH being the dominant product. By conducting a systematic exploration of operating parameters including applied current density, applied CO_2 pressure, cation effect, and electrolyte concentration, the selectivity towards formate (HCOOH) is optimized, achieving a remarkable 70 % faradaic efficiency (FE) under moderate conditions of 25 bar in a 0.5 M cesium bicarbonate ($CsHCO_3$) electrolyte. Additionally, we report the synthesis of isopropanol with a FE of 11 % at the 25 bar in 0.5 M $KHCO_3$ which is the highest reported selectivity towards isopropanol on copper using a bicarbonate system.

1. Introduction

Striving for carbon neutrality remains a worldwide ambition in mitigating climate change as global temperatures continue to rise with each passing year [1]. The electrochemical CO_2 reduction reaction (CO_2RR) has received ample interest as a potential power-to-chemical technology [2]. Its main advantages are the possibility to produce a wide range of useful products and the relatively mild process conditions. Many promising catalysts have been identified for CO_2RR, which are typically classified based on their selectivity towards different products [3,4]. Among these, copper is the only known catalyst that produces a blend of hydrocarbons, alcohols, and aldehydes directly from CO_2 [56]. Yet, the CO_2RR on copper suffers from a limited product selectivity [6–9].

A challenge that pertains to the CO_2RR is the poor solubility of CO_2 in aqueous electrolytes (~33 mM in water [10]). This results in poor conversion rates and limits CO_2 reduction selectivity due to the competition with the hydrogen evolution reaction (HER) in the same potential window. One interesting way of increasing the CO_2 concentration is by increasing the amount of dissolved CO_2 using elevated pressures [11–14]. Pressurizing CO_2 into the electrolyte has been reported to enhance the CO_2RR by improving the selectivity and partial current densities towards CO_2 reduction products [13–16], while pressurizing in general could enable better integration of the CO_2RR with upstream and downstream operations [17]. Additionally, it offers the chance to work at increased temperatures, given that higher temperatures result in decreased CO_2 solubility, potentially benefiting reaction kinetics [18]. Recent studies suggest that the CO_2 reduction reaction (CO_2RR) performance can be modified by manipulating the operating pressure. The catalytic performance is altered through multiple mechanisms, for instance through changing thermodynamics of the reaction, balance of the carbonate buffer reactions ($CO_2/HCO^{3-}/CO_3^{2-}$), and the extent of CO_2 coverage and coverage of reaction intermediates on the catalyst surface [19–21]. The rate of CO_2RR has also been shown to diminish below a pressure of 1 atm while H_2 evolution dominates [22]. Recently, Lamaison et al. reported a boost in the CO partial current density to −286 $mA.cm^{-2}$ at a CO_2 pressure of 9.5 atm on an Ag-Zn alloy dendrite catalyst that was well above its mass transport limited current density of −30 mA cm^{-2} at 1 atm [23]. Hashiba et at., reported a boost in the synthesis of CH_4 with a stable suppression of H_2 evolution at elevated CO_2 pressures [24]. In a recent study by Ramdin et al., formate selectivity was increased to 90 % with a $j > 30$ $mA.cm^{-2}$ at a pressure of 50 bar [25]. Even with these promising results, there is still very limited research on high-pressure CO_2RR, with most studies focusing on the

* Corresponding author.
E-mail address: r.kortlever@tudelft.nl (R. Kortlever).

https://doi.org/10.1016/j.cej.2024.150478
Received 22 November 2023; Received in revised form 21 February 2024; Accepted 15 March 2024
Available online 16 March 2024

production of C_1 products such as CO and formic acid on metallic electrodes such as silver, gold, and tin [12,26–30].

In contrast, only a handful of studies have investigated elevated pressure CO_2RR on copper electrodes in aqueous electrolytes. These studies have been, for the most part, restricted to flat planar electrodes in autoclave type reactors [31–34]. For example, a recent study by Li et al. using a (1 1 1) oriented Cu_2O film on a copper foil reported a high FE_{HCOOH} of 98 % at a high CO_2 pressure of 60 atm [33]. A more recent study by Huang et al., reported a 84 % formate FE at 50 bar CO_2 pressure using a polypyrrole-coated copper (CuPPy) electrode. While these studies show the potential of using a pressurized CO_2 feed to achieve high product selectivities using tailor made catalysts, yet they do so at extreme pressure conditions (≥50 bar). However, recent studies have shown that using moderate pressures up to 25 bar is beneficial as it involves low operational and capital costs [35,36]. To the best of our knowledge, there are very limited studies performed on the electrochemical CO_2RR performance of copper in this operating pressure window of 1–25 bar.

Therefore, we here report a systematic study on the influence of pressure on a polished copper foam electrode in a custom built flow cell [11]. The effect of different operating parameters, including, applied current density, cation size and electrolyte concentration, is investigated. We show that the coupled use of pressurized CO_2 and Cu foam electrode offers a notable improvement in the formate selectivity while unlocking new C-C coupled pathways towards higher alcohols.

2. Experimental section

2.1. Materials

An ultrapure water purification system (MilliQ IQ 7000, Merck–Millipore, USA) was used as water source for all experiments. Potassium and cesium bicarbonate ($KHCO_3$, ≥ 99.95 % trace metals basis, 99.7–100.5 % dry basis, and $CsHCO_3$ 99.9 %, metals basis, Sigma Aldrich) were used to prepare 0.5, 1, and 2 M catholytes. 1 M potassium hydroxide (KOH pellets, ACS reagent, Emsure) was used as the anolyte. The working electrode used for electrochemical experiments was a copper foam (99.8–99.9 %, Recemat BV) and nickel foam (99.9 %, Recemat BV) served as the counter electrode. Nafion 117 (Ion Power GmbH) was cleaned in MilliQ water and used as the ion exchange membrane. Hydrochloric acid (ACS reagent, 37 %, Sigma Aldrich), acetone (Technical Grade, assay ≥ 99 %, VWR Chemicals) and phosphoric acid (85 % VLSI, Technic) were used for cleaning and preparation of the electrodes. Sulfuric acid (95–97 %, ACS reagent, Honeywell), DMSO (ACS reagent, ≥99.9 %, Sigma Aldrich), phenol (ACS reagent, 99.0–100.5 %, Sigma Aldrich), and D_2O (99.9 atom% D, Sigma Aldrich) were used for liquid product analysis. All reagents were used without further purification.

2.2. Electrochemical measurements

The electrochemical performance of the copper foam electrodes at different pressures were assessed using chronopotentiometry experiments by applying current densities and measuring the potentials. Chronopotentiometry was employed because recent studies have demonstrated notable changes in the immediate surroundings near the catalyst surface based on the current density [37]. Consequently, in this context, we aim to investigate how these changes might influence product selectivity. A custom made flow cell with a continuous gas product measurement and stackable clamp design was used to conduct the experiments, as detailed in our previous work [11]. In brief, the setup was designed with flexibility and ease of operation in mind and can handle pressures up to 50 bar while functioning in a continuous mode including inline gas product analysis. A Biologic BP300 potentiostat was used for all CO_2RR experiments. Nickel foam and a miniaturized leakless Ag/AgCl reference electrode (LF 1.6–45 mm, Innovative Instruments, Inc., USA) served as the anode and reference electrode respectively. 0.5, 1 or 2 M $KHCO_3$ or $CsHCO_3$ was used as the catholyte while 1 M KOH was used as the anolyte. The cathode and anode chambers were separated using a Nafion 117 membrane. Before each experiment the catholyte was purged with CO_2 at the desired pressure in an external reservoir for 30 min (for schematics of the setup, please see Fig. S1). The CO_2RR was performed at ambient temperature and at four different gas pressures; 1, 5, 10, and 25 bar. The reactor pressure was held slightly higher (≥5 bar) compared to the gas pressure to prevent dissolved gases from escaping the electrolyte due to ohmic heating near the electrode. Also, having a higher upstream pressure on the back pressure regulator helps with quicker discharge of dissolved gases into the headspace as the circulated electrolyte enters the reservoir.

2.3. Electrode preparation

For each experiment a freshly cut copper and nickel foam electrode was used. Images of the copper foam electrode at different stages in the experimental procedure are depicted in Fig. 1. Copper foam was cut in the shape of a cylinder with a diameter of 1 cm and thickness of 0.4 cm. Prior to each experiment the copper foam was first sonicated in acetone for 10 min followed by washing with 2 M HCl for 5 min. Afterwards it was rinsed with ultrapure water and dried under argon flow, before putting it in a two electrode electrochemical cell [38], where it was electropolished in 85 % phosphoric acid using a carbon rod as counter and reference electrode by applying a potential of 2.1 V for 4 min. A similar cleaning procedure was performed on the nickel foam except for the electropolishing step.

2.4. Characterization

Scanning Electron Microscopy (SEM, Jeol JSM 6500F) images were taken prior and after the experiments to understand the changes incurred to the copper foam during the experiment. An energy dispersive X-ray spectrometry detector (Ultradry, Thermofischer, *USA*) enabled detection of chemical elemental composition. X-Ray Diffraction (XRD) patterns were obtained using a Bruker D8 Advance diffractometer (Bruker, *USA*) Bragg-Brentano geometry with graphite monochromator and Vantec position sensitive detector (Co Kα radiation. Divergence slit var12, scatter screen height 8 mm, 40 kV 40 mA).

The surface chemistry of the electrodes was studied using a Thermo Scientific™ K-Alpha™ spectrometer (Thermoscientific, *USA*). The monochromated aluminum Kα radiation, with a photon energy of 1486.7 eV, was used to generate a monochromated X-ray with a spot size of 400 μm. The X-ray photoelectron spectroscopy (XPS) data were acquired before and after the experiments. To compensate for the differential charging, a flood gun was employed. High-resolution scans were acquired with a step size of 0.1 eV. The XPS spectra obtained were analysed using the CasaXPS software.

3. Results and discussion

3.1. Effect of pressure and current density on CO_2 electroreduction

The influence of pressure on the CO_2RR on copper foam electrodes (ECSA = 3.3 cm^2 (see S4)) was studied using the previously described

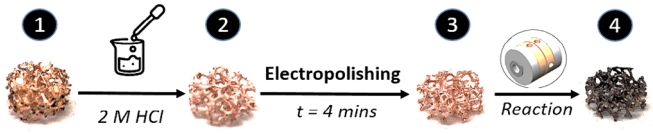

Fig. 1. Images of the copper foam electrode at different stages in the experimental procedure: (1) as received, (2) After a 2 M HCl acid wash, (3) after electropolishing in phosphoic acid, (4) after electrochemical CO_2 reduction.

cell at different applied current densities (j) (Fig. 2). As a base case, a pressure of 1 bar of CO_2 was applied and the electrochemical performance was measured at −30, −40, −50, and −60 mA (j = -9.1, −12.1, −15.2, and −18.2 mA/cm^2). H_2 is the dominating product at all applied current densities with the $FE_{H2} > 70$ %. The main CO_2RR products observed are formate (HCOOH), methane (CH_4), ethylene (C_2H_4) and carbon monoxide (CO), with a combined FE < 30 %. This relatively poor performance is explained by the poor CO_2 solubility in aqueous electrolytes at 1 bar. Remarkably, at the highest pressure studied in this work (25 bar), the trend is reversed with CO_2RR products reaching a total FE > 70 % at the expense of hydrogen production, which is suppressed to less than 30 % (see section S9 for details regarding all the products). It is interesting to note that with an increase in pressure from 1 to 10 bar, the most preferred CO_2RR product is HCOOH followed by CO, while we only observe trace amounts of ethylene at higher current densities. However, at 25 bar, apart from HCOOH and CO, the most preferred products are oxygenates (alcohols) with trace amounts of hydrocarbons.

To rule out that differences in observed CO_2RR performance arise from catalyst morphology and compositional changes, we performed characterizations prior to and after electrochemical measurements. The surface morphology of the used copper foam electrodes, as visualized with SEM, does not exhibit any substantial changes to the electrodes prior to the experiment (S5). Similarly, XRD measurements show no changes in the crystal structures of the copper foam post electrochemical measurements (S8). The copper foam is polycrystalline in nature with the most dominant facets being Cu(1 0 0) and Cu(1 1 1)[39]. This also dismisses any contributions to the observed performance due to changes in the catalyst crystal structure. The deconvoluted XPS C 1s and Cu 2p spectra for pure copper foam and after experiments at 5 bar, 10 bar, and 25 bar are shown in supplementary information S6 and S7. We mainly observe that after the electrochemical experiments trace amounts of various carbon species are present on the copper surface. In situ XPS studies on copper during CO_2 reduction have reported the formation of carbon species (specifically via the C_1 pathway) [40]. Previous studies have shown that the formation of carbon mainly occurs in bicarbonate systems and surfaces with less defects (polished electrodes) [41].

At 25 bar, HCOOH is the favoured product at all current densities with the highest FE_{HCOOH} of ~ 57 % at −9.1 mA/cm^2. With more negative current densities at 25 bar, there is a decline in HCOOH production with a simultaneous increase in FE_{H2} and FE_{CO}. The initial step in the CO_2RR is believed to be the formation of a carboxylate intermediate $*CO_2^-$ anion radical [7,42,43],

$$CO_2 + e^- \rightarrow *CO_2^- \quad (1)$$

which can bind to the copper surface through either C, O, both O's, or both C and O [44,45]. The formation of HCOOH occurs through either a hydride or proton coupled electron transfer (PCET) reaction when $*CO_2^-$ is bound with a C or O atom to the copper surface, as demonstrated in the following equations:

$$*CO_2^- + *H \rightarrow HCOO^- \quad (2)$$

$$*CO_2^- + H^+ + e^- \rightarrow HCOO^- \quad (3)$$

$$*CO_2^- + H^+ + e^- \rightarrow COOH^- \quad (4)$$

$$*CO_2^- \rightarrow * CO + *O^- \quad (5)$$

Irina et al. suggest that the reaction proceeds via the carboxylate intermediate (–CO_2^-), which is stabilized on the electrode surface due to an interplay of its electrostatic interactions with the hydrated metal cations, strong covalency of the carbon atom towards the surface, and the polarization forces present near the electrode [46]. Further cathodic activation (applying more negative currents/potentials) results in the weakening of the C-Cu bond and C-O bond, with simultaneous

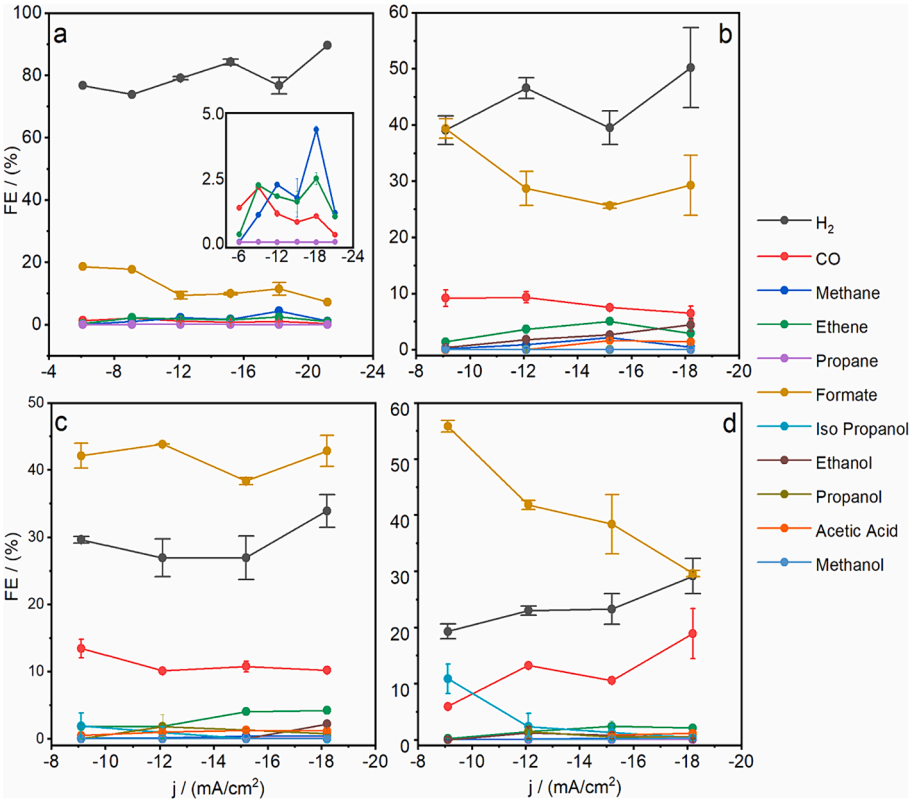

Fig. 2. Faradaic efficiency towards product at varying applied current densities at a) 1 bar, b) 5 bar, c) 10 bar, and d) 25 bar CO_2 pressure using a Cu foam in a 0.5 M $KHCO_3$ electrolyte. The exact faradaic efficiency values can be found in supplementary section S9.

stabilization of the O-Cu bond. At this stage, either step (2) or (3) can result in the formation of $HCOO^-$ or direct formation of CO with further protonation (this is true for near neutral or alkaline conditions). Another possibility is the interaction between a proton and the exposed O atom of the $*CO_2^-$ anion radical giving rise to a carboxyl intermediate (step 4), which can lead to both CO and $HCOO^-$ [47]. Recent studies on copper catalysts indicate that the HCOOH pathway is favoured on Cu (1 1 1) [46] and Cu (2 0 0) surfaces [48]. The increase in HCOOH production with increasing pressure has been recently reported and is ascribed to an increase in CO_2 coverage [34,49] with a simultaneous drop in surface water coverage that serves as the main proton donor [50]. The formation of HCOOH requires the least protons per carbon atom among the different liquid products which explains its increased formation relative to more hydrogenated CO_2RR products.

The shift in selectivity from HCOOH to CO and subsequently to hydrocarbons as the cathodic current density increases is attributed to a transition from a thermodynamics to a kinetics-mediated pathway [51]. Another crucial factor to consider is the interfacial pH, which affects the pathways towards HCOOH and CO differently. This becomes particularly evident at 25 bar (Fig. 2d) when the current density is increased from −9.1 to −18.2 mA/cm^2, resulting in an increase in CO production, with a decline in FE_{HCOOH}, and a simultaneous increase in H_2 formation. This observation is explained by the interplay between the flux of CO_2 (concentration in the bulk) and the pH at the electrode surface, that increases with increasing current densities [32]. At −18.2 mA/cm^2, reducing the pressure from 25 bar to 1 bar follows a volcano like trend for C_{2+} species, with the FE peaking at 5 bar for ethylene and 10 bar for ethanol (S9). This can be attributed to the fact that at 25 bar, there is a higher amount of CO_2 available to react with the generated OH^- ions at the electrode surface, effectively buffering the interfacial pH. However, as the pressure decreases, the concentration of CO_2 (and consequently the CO_2 flux to the surface) diminishes, leading to a weaker pH buffering effect. Additionally, the presence of a higher amount of surface water [50] at lower pressures compared to higher pressures contributes to an increased amount of adsorbed hydrogen on the electrocatalytic surface, promoting the formation of more reduced products from CO_2.

Interestingly, we observe the formation of isopropanol (IPA) at 10 bar and 25 bar. The FE_{IPA} peaks at ~ 11 % when applying 25 bar and −9.1 mA/cm^2 and drops to a mere 0.7 % at −18.2 mA/cm^2 (Fig. 2d). Isopropanol is an uncommon product for CO_2RR on copper electrodes as it requires the transfer of 18 electrons:

$$3CO_2 + 18\,H^+ + 18\,e^- \rightarrow C_3H_8O + 5H_2O \quad (6)$$

Although the exact mechanism behind the formation of isopropanol on copper is still unclear, a possible pathway is explained below based on our experimental results and the mechanistic studies conducted by Garcia et al. [52] and Kun et al. [53]. *CO species (equation (1) can dimerize via a C-C coupling following an initial electron transfer and a proton transfer to give a reduced dimer species (*CO-COH) which can rearrange and reduce further to give rise to a C_2 enol intermediate (*C_2H_3O, a precursor to ethanol). At the lower current densities, a higher surface *CO density, that occurs at higher pressures, can promote interactions between the enol intermediate with adjacent *CO species. Further proton coupled electron transfers then result in the formation of a C_3 enol species that can give rise to isopropanol mimicking the pathway of ethanol formation from the C_2 enol intermediate. The low amounts of ethanol at all tested conditions (especially at higher pressures) are assumed to be due to its consumption at the copper electrode to produce isopropanol.

To provide a general understanding, the reader is guided through the trends in FE_{IPA}, FE_{CO} and FE_{EtOH} below. When the current density is increased (going from −9.1 to −18.2 mA/cm^2) at a pressure of 25 bar, a gradual rise in FE_{CO} is observed, while FE_{EtOH} initially rises to 0.8 % before dropping to 0.3 %. At the same time, as the current density becomes more negative, FE_{IPA} decreases from 11 % to zero. Notably, at

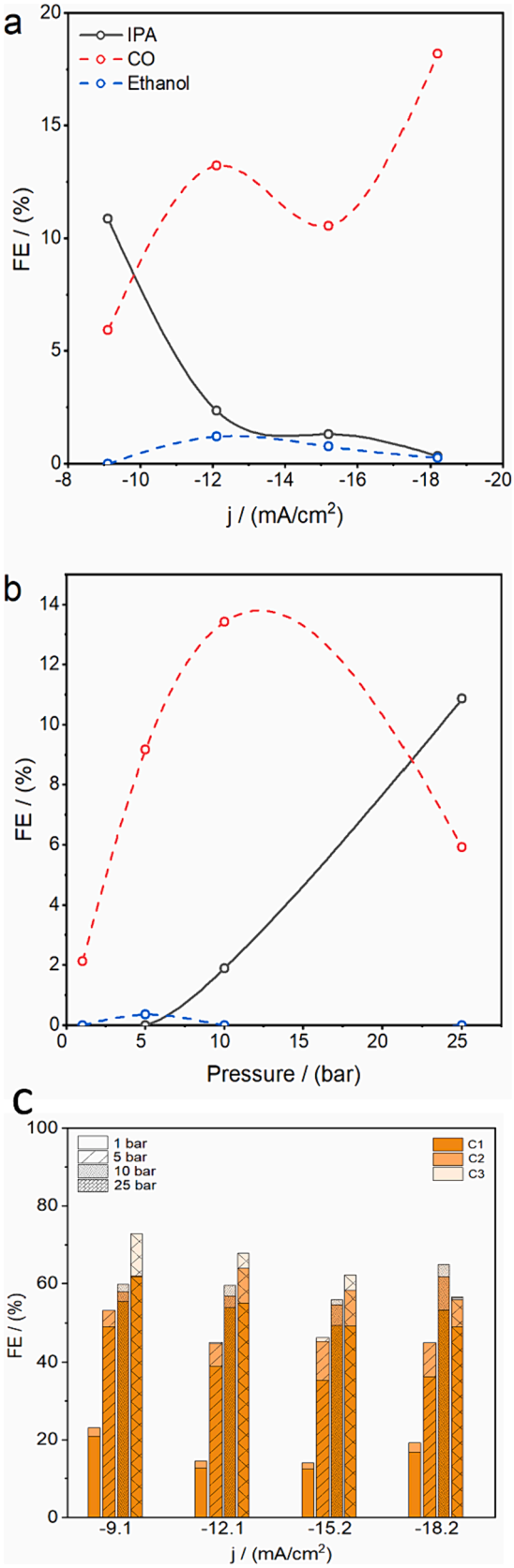

Fig. 3. A) relationship between fe_{IPA}, FE_{CO}, and FE_{EtOH} versus applied current densities at P = 25 bar, b) Relationship between FE_{IPA}, FE_{CO}, and FE_{EtOH} versus CO_2 pressure at j = -9.1 mA/cm^2, c) C_1, C_2 and C_3 product FE versus applied current densities under PCO2 = 1, 5, 10, and 25 bar. All experiments were carried out in 0.5 M $KHCO_3$ (For error bars see Fig. 2 and Fig. S9).

−9.1 mA/cm^2, where the most isopropanol is observed (as shown in Fig. 3a), ethanol is not detected. This is similar to the results reported by Kun et al., where an increase in FE_{IPA} was observed at the expense of FE_{EtOH} and FE_{CO} [53]. Also, at −9.1 mA/cm^2, there is an initial increase in CO production when the pressure is raised from 1 bar, which then decreases to about 5.9 % as the pressure reaches 25 bar (Fig. 3b). A similar pattern is seen for FE_{EtOH}. Alongside this, FE_{IPA} shows an opposite trend to that of FE_{CO} and FE_{EtOH}, increasing from 1.9 % at 10 bar to 11 % at 25 bar.

A broad overview of the trends in total C_1, C_2, and C_3 product distributions over the entire range of applied current densities under different CO_2 pressures is shown in Fig. 3c. Furthermore, the partial current densities of HCOOH, CO and H_2 versus applied current densities at all pressures are provided in the supplementary section S14.

3.2. Effect of cation at elevated pressure

An interesting parameter to consider is the cation effect that has a substantial impact on the electrochemical CO_2 reduction performance at ambient pressures. In fact, a recent study by Monteiro et al., claimed the absence of any CO_2 reduction on Ag, Au and Cu electrodes without cations [54]. While the exact mechanism is still debated, previous studies have demonstrated that larger cations like Cs^+ can boost CO_2RR activity by inducing changes to the local pH [55], the interfacial electric field close to the electrode surface [56,57], stabilizing various reaction intermediates [58], or by modifying the structure of surface bound water [59]. While these studies have been mainly restricted to ambient pressures, combining these effects with the increased CO_2 concentrations at high pressures, could lead to further selectivity enhancements. To probe this, experiments were carried out to investigate the influence of cation size toward CO_2 reduction performance (at 25 bar, −9.1 and −18.2 mA/cm^2) using a 0.5 M $CsHCO_3$ electrolyte.

The selectivities towards CO, H_2, and formate as a function of cation choice are shown in Fig. 4. Isopropanol has been omitted as it was not present while using 0.5 M $CsHCO_3$ at either of the studied current densities. The results presented in Fig. 4 show that there is not a significant difference in FE_{HCOOH} at −9.1 mA/cm^2 between K^+ and Cs^+, with only a slight increase observed with K^+ (FE_{HCOOH} = 55 % compared to 51 % for Cs^+). However, at −18.2 mA/cm^2, the FE of HCOOH increases significantly from approximately 30 % for $KHCO_3$ to 70 % for $CsHCO_3$, more than doubling in value. Moreover, the production of hydrogen is suppressed to 10 %. Cations with a smaller hydration shell such as Cs^+ have been shown to be more concentrated at the electrode surface under reduction conditions than cations such as K^+ with a bigger hydration radius, [56]. Mechanistic studies at ambient pressure also report that Cs^+ can stabilize negatively charged reaction intermediates such as $*CO_2^-$ (a common precursor to both HCOOH and CO [47]) much more strongly than K^+ [54]. Here, the interplay of the above

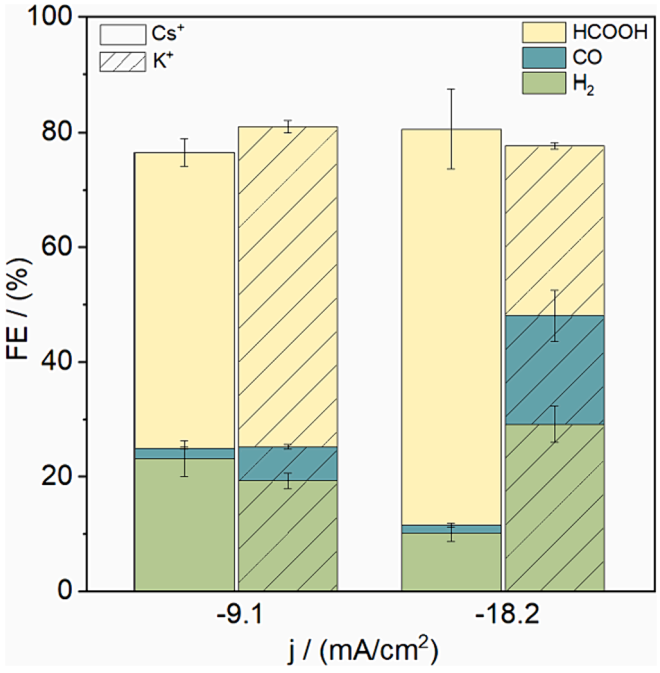

Fig. 4. FE of H_2, CO, and HCOOH versus current density (-9.1 and −18.2 mA/cm^2) at P = 25 bar in 0.5 M $KHCO_3$ and $CsHCO_3$.

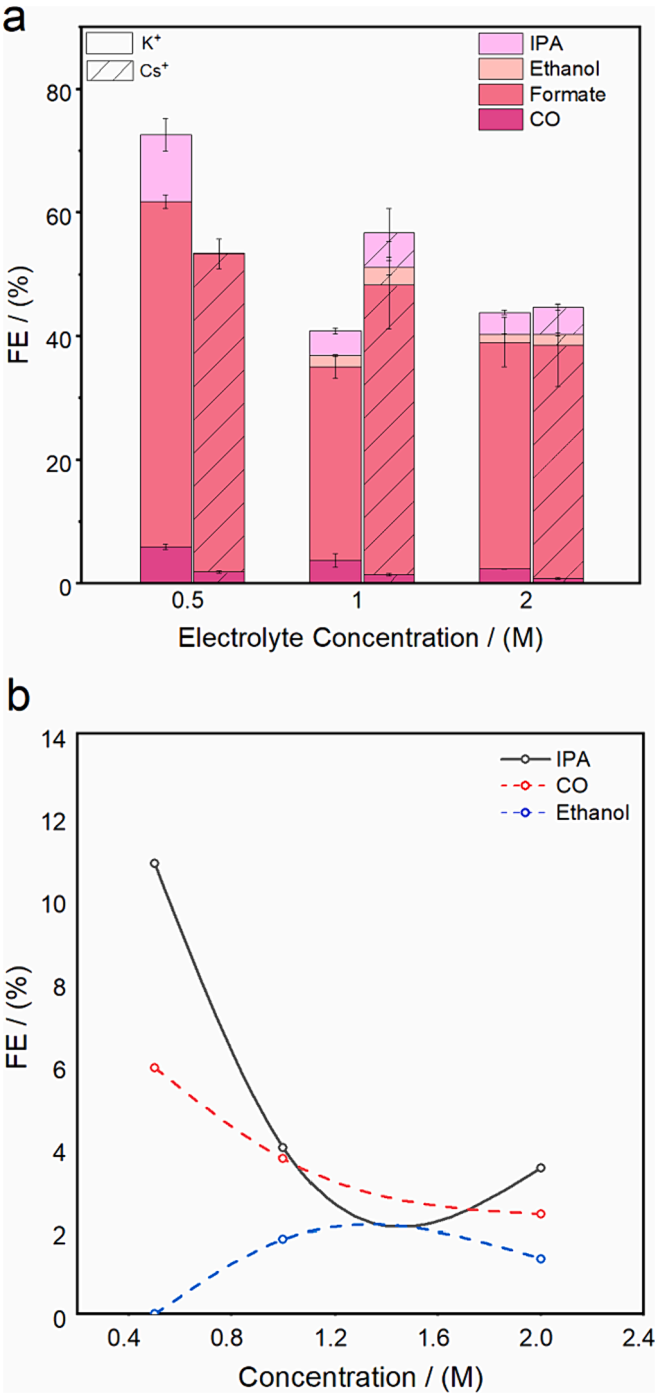

Fig. 5. A) fe of co, ethanol, hcooh, and isopropanol versus electrolyte concentration (0.5, 1, and 2 M) at P = 25 bar and −9.1 mA/cm^2, b) Relationship between FE_{IPA}, FE_{CO}, and FE_{EtOH} versus $KHCO_3$ concentration at j = -9.1 mA/cm^2 and P = 25 bar.

enhancement effects of Cs^+ combined with the increased concentrations of CO_2 at high pressure explains the notable increase in the selectivity and partial current density towards HCOOH.

3.3. Effect of electrolyte concentration at elevated pressure

The CO_2 electrochemical reduction activity was further investigated by studying the effects of electrolyte concentration with 0.5, 1 M and 2 M $KHCO_3$ and $CsHCO_3$ at 25 bar and −9.1 mA/cm^2 (Fig. 5a). The motivation behind these experiments was to understand the impact of electrolyte concentration on the reduction activity as studies at ambient pressure have shown that the [CO_2]/[cation] ratio can have a significant impact on the performance of a copper electrode [60]. The major factors dictating the observed behaviour are a loss of CO_2 to the salting out effect, a decrease in local pH due to the stronger buffering effect of a higher bicarbonate concentration, a drop in the electric field affecting the stability of CO_2RR intermediates, and an increased CO_2 mass transport limitation due to the adsorption of cations on the electrode surface owing to an increased cation/[CO_2] ratio. According to Ramdin et al. [14], a moderate electrolyte concentration exists that works best for high pressure CO_2 reduction to formic acid.

Fig. 5a shows that the FE_{HCOOH} decreases with an increase in concentration for both the electrolytes ($KHCO_3$ and $CsHCO_3$). Interestingly, there is a decline in FE_{CO} and FE_{IPA} when increasing the electrolyte concentration from 0.5 to 2 M with a simultaneous increase in FE_{EtOH} reaching a maximum value of 1.8 % at 1 M before decreasing to 1.3 % for 2 M. The decrease in FE_{CO} can be attributed to the decrease in local interfacial pH (though less significant at higher pressure) with an increase in electrolyte (therefore, [HCO_3^-]) concentration, which also results in slightly higher amounts of H_2 and CH_4 (see supporting information S10). The trends shown in Fig. 5b, for the different $KHCO_3$ concentrations, further illustrate that the variation in FE_{IPA} is closely tied to the changes in FE_{CO} and FE_{EtOH}, similar to the patterns presented in Fig. 3a and b. This emphasizes the existence of a pathway towards isopropanol that mimics ethanol formation [41].

For $CsHCO_3$, the trends for FE_{HCOOH}, FE_{CO}, and FE_{EtOH} are like that of $KHCO_3$, however there are some notable differences. The ethanol selectivity increases from 0.1 % for 0.5 M to 2.9 % for 1 M $CsHCO_3$ before dropping to 1.8 % at 2 M. Moreover, the amount of CO is lower at all the studied $CsHCO_3$ concentrations while isopropanol only appears at 1 M concentration indicating a different optimum for Cs^+ compared to K^+.

4. Conclusions

We report a systematic investigation of the effects of pressure, current density, cation size, and electrolyte concentration on the electrochemical CO_2 reduction using a copper foam electrode. At 25 bar, the electrode shows a remarkable selectivity of 70 % for formate in 0.5 M $CsHCO_3$ with j_{HCOOH} of −12.7 mA/cm^2. Furthermore, we report the formation of the uncommon product – isopropanol, with a FE of 11 % in 0.5 M $KHCO_3$ at 25 bar, which is the highest reported selectivity for this product under moderate pressures on a polished copper foam. The conducted experiments shed light on the idea that electrolyte engineering coupled with the right operating conditions can be a viable option to enhance the selectively towards profitable products such as formate on a simple copper electrode [61]. Moreover, a pressurized CO_2 feed can potentially unlock new C-C coupling pathways on copper and pave the way towards the production of elusive higher CO_2 reduction products. This also questions whether newly developed catalysts should be tested under elevated pressure conditions.

5. Ethic Declaration

All authors have given approval to the final version of the manuscript and declare no competing financial interests that could have influenced the work reported here.

Funding

This study is part of the “Reactor, Process and System Design” project of the Electrons to Chemical Bonds (E2CB) consortium, which is financed by NWO via the Perspective programme and affiliated industrial partners under the project number P17-08.

CRediT authorship contribution statement

Nandalal Girichandran: Writing – original draft, Methodology, Investigation, Conceptualization. **Saeed Saedy:** Writing – review & editing, Investigation. **Ruud Kortlever:** Writing – review & editing, Supervision, Methodology, Funding acquisition, Conceptualization.

Declaration of competing interest

The authors declare that they have no known competing financial interests or personal relationships that could have appeared to influence the work reported in this paper.

Data availability

Data will be made available on request.

Acknowledgements

The authors would like to thank Michel van den Brink for his support in the laboratory and Ruud Hendrikx for help with XRD. The authors would also like to thank Dr. Andrew Morrison for fruitful discussions.

Appendix A. Supplementary data

Supplementary data to this article can be found online at https://doi.org/10.1016/j.cej.2024.150478.

References

[1] Global Warming of 1.5 °C —, (n.d.). https://www.ipcc.ch/sr15/ (accessed July 4, 2023).
[2] J. Wyndorps, H. Ostovari, N. von der Assen, Is electrochemical CO2 reduction the future technology for power-to-chemicals? an environmental comparison with H2-based pathways, sustain, Energy Fuels 5 (2021) 5748–5761, https://doi.org/10.1039/D1SE00975C.
[3] M.G. Kibria, J.P. Edwards, C.M. Gabardo, C.T. Dinh, A. Seifitokaldani, D. Sinton, E. H. Sargent, Electrochemical CO2 reduction into chemical feedstocks: from mechanistic electrocatalysis models to system design, Adv. Mater. 31 (2019), https://doi.org/10.1002/adma.201807166.
[4] Y. Pei, H. Zhong, F. Jin, A brief review of electrocatalytic reduction of CO2—Materials, reaction conditions, and devices, Energy Sci. Eng. (2021) 1012–1032, https://doi.org/10.1002/ese3.935.
[5] Y. Hori, K. Kikuchi, S. Suzuki, Production of CO and CH4 in electrochemical reduction of CO2 at metal electrodes in aqueous hydrogencarbonate solution, Chem. Lett. 14 (1985) 1695–1698, https://doi.org/10.1246/CL.1985.1695.
[6] K.P. Kuhl, E.R. Cave, D.N. Abram, T.F. Jaramillo, New insights into the electrochemical reduction of carbon dioxide on metallic copper surfaces, energy, Environ. Sci. 5 (2012) 7050–7059, https://doi.org/10.1039/c2ee21234j.
[7] M. Gattrell, N. Gupta, A. Co, A review of the aqueous electrochemical reduction of CO2 to hydrocarbons at copper, J. Electroanal. Chem. 594 (2006) 1–19, https://doi.org/10.1016/j.jelechem.2006.05.013.
[8] S. Asperti, R. Hendrikx, Y. Gonzalez-Garcia, R. Kortlever, Benchmarking the electrochemical CO2 reduction on polycrystalline copper foils: the importance of microstructure versus applied potential, ChemCatChem 14 (2022) e202200540.
[9] S. Nitopi, E. Bertheussen, S.B. Scott, X. Liu, A.K. Engstfeld, S. Horch, B. Seger, I.E. L. Stephens, K. Chan, C. Hahn, J.K. Nørskov, T.F. Jaramillo, I. Chorkendorff, Progress and perspectives of electrochemical CO2 reduction on copper in aqueous electrolyte, Chem. Rev. 119 (2019) 7610–7672, https://doi.org/10.1021/acs.chemrev.8b00705.
[10] J. Li, J. Guo, H. Dai, Probing dissolved CO2(aq) in aqueous solutions for CO2 electroreduction and storage, Sci. Adv. 8 (2022), https://doi.org/10.1126/sciadv.abo0399.

[11] A.R.T. Morrison, N. Girichandran, Q. Wols, R. Kortlever, Design of an elevated pressure electrochemical flow cell for CO2 reduction, J. Appl. Electrochem. 1 (2023) 1–10, https://doi.org/10.1007/S10800-023-01927-7/FIGURES/8.
[12] F. Proietto, B. Schiavo, A. Galia, O. Scialdone, Electrochemical conversion of CO2 to HCOOH at tin cathode in a pressurized undivided filter-press cell, Electrochim. Acta 277 (2018) 30–40, https://doi.org/10.1016/j.electacta.2018.04.159.
[13] F. Proietto, S. Li, A. Loria, X.M. Hu, A. Galia, M. Ceccato, K. Daasbjerg, O. Scialdone, High-pressure synthesis of CO and syngas from CO2 reduction using Ni−N-doped porous carbon electrocatalyst, Chem. Eng. J. 429 (2022) 132251, https://doi.org/10.1016/j.cej.2021.132251.
[14] M. Ramdin, A.R.T. Morrison, M. De Groen, R. Van Haperen, R. De Kler, E. Irtem, A. T. Laitinen, L.J.P. Van Den Broeke, T. Breugelmans, J.P.M. Trusler, W. De Jong, T. J.H. Vlugt, High-pressure electrochemical reduction of CO2 to formic acid/formate: effect of pH on the downstream Separation process and economics, Ind. Eng. Chem. Res. 58 (2019) 22718–22740, https://doi.org/10.1021/acs.iecr.9b03970.
[15] Y. Hiejima, M. Hayashi, A. Uda, S. Oya, H. Kondo, H. Senboku, K. Takahashi, Electrochemical carboxylation of α-chloroethylbenzene in ionic liquids compressed with carbon dioxide, PCCP 12 (2010) 1953–1957, https://doi.org/10.1039/B920413J.
[16] S. Messias, M.M. Sousa, M. Nunes Da Ponte, C.M. Rangel, T. Pardal, A.S. R. MacHado, Electrochemical production of syngas from CO2 at pressures up to 30 bar in electrolytes containing ionic liquid, React. Chem. Eng. 4 (2019) 1982–1990, https://doi.org/10.1039/C9RE00271E.
[17] B.F. Snyder, M. Layne, D.E. Dismukes, A cash flow model of an integrated industrial CCS-EOR project in a petrochemical corridor: a case study in Louisiana, Int. J. Greenhouse Gas Control 93 (2020) 102885, https://doi.org/10.1016/J.IJGGC.2019.102885.
[18] F. Proietto, R. Rinicella, A. Galia, O. Scialdone, Electrochemical conversion of CO2 to formic acid using a sn based cathode: combined effect of temperature and pressure, J. CO2 Util. 67 (2023) 102338, https://doi.org/10.1016/J.JCOU.2022.102338.
[19] K. Hara, A. Tsuneto, A. Kudo, T. Sakata, Change in the product selectivity for the electrochemical CO2 reduction by adsorption of sulfide ion on metal electrodes, J. Electroanal. Chem. 434 (1997) 239–243, https://doi.org/10.1016/S0022-0728(97)00045-4.
[20] Y. Hori, H. Wakebe, T. Tsukamoto, O. Koga, Electrocatalytic process of CO selectivity in electrochemical reduction of CO2 at metal electrodes in aqueous media, Electrochim. Acta 39 (1994) 1833–1839, https://doi.org/10.1016/0013-4686(94)85172-7.
[21] J.J. Carroll, J.D. Slupsky, A.E. Mather, The solubility of Carbon dioxide in water at low pressure, J. Phys. Chem. Ref. Data 20 (1991) 1201–1209, https://doi.org/10.1063/1.555900.
[22] G.Z. Kyriacou, A.K. Anagnostopoulos, Influence CO2 partial pressure and the supporting electrolyte cation on the product distribution in CO2 electroreduction, J. Appl. Electrochem. 23 (1993) 483–486, https://doi.org/10.1007/BF00707626/METRICS.
[23] S. Lamaison, D. Wakerley, J. Blanchard, D. Montero, G. Rousse, D. Mercier, P. Marcus, D. Taverna, D. Giaume, V. Mougel, M. Fontecave, High-current-density CO2-to-CO electroreduction on ag-alloyed zn dendrites at elevated pressure, Joule 4 (2020) 395–406, https://doi.org/10.1016/j.joule.2019.11.014.
[24] H. Hashiba, S. Yotsuhashi, M. Deguchi, Y. Yamada, Systematic analysis of electrochemical CO_2 reduction with Various reaction Parameters using combinatorial reactors, ACS Comb. Sci. 18 (2016) 203–208, https://doi.org/10.1021/ACSCOMBSCI.6B00021.
[25] M. Ramdin, A.R.T. Morrison, M. De Groen, R. Van Haperen, R. De Kler, L.J.P. Van Den Broeke, J.P. Martin Trusler, W. De Jong, T.J.H. Vlugt, High pressure electrochemical reduction of CO2 to formic acid/formate: a Comparison between Bipolar membranes and cation exchange membranes, Ind. Eng. Chem. Res. 58 (2019) 1834–1847, https://doi.org/10.1021/ACS.IECR.8B04944/ASSET/IMAGES/MEDIUM/IE-2018-04944D_M012.GIF.
[26] O. Scialdone, A. Galia, G. Lo Nero, F. Proietto, S. Sabatino, B. Schiavo, Electrochemical reduction of carbon dioxide to formic acid at a tin cathode in divided and undivided cells: effect of carbon dioxide pressure and other operating parameters, Electrochim. Acta 199 (2016) 332–341, https://doi.org/10.1016/J.ELECTACTA.2016.02.079.
[27] F. Proietto, F. Berche, A. Galia, O. Scialdone, Electrochemical conversion of pressurized CO2 at simple silver-based cathodes in undivided cells: study of the effect of pressure and other operative parameters, J. Appl. Electrochem. 51 (2021) 267–282, https://doi.org/10.1007/S10800-020-01505-1/FIGURES/6.
[28] C.M. Gabardo, A. Seifitokaldani, J.P. Edwards, C.T. Dinh, T. Burdyny, M.G. Kibria, C.P. O'Brien, E.H. Sargent, D. Sinton, Combined high alkalinity and pressurization enable efficient CO2 electroreduction to CO, energy, Environ. Sci. 11 (2018) 2531–2539, https://doi.org/10.1039/C8EE01684D.
[29] E.J. Dufek, T.E. Lister, S.G. Stone, M.E. McIlwain, Operation of a pressurized system for continuous reduction of CO 2, J. Electrochem. Soc. 159 (2012) F514–F517, https://doi.org/10.1149/2.011209JES/XML.
[30] M. Todoroki, K. Hara, A. Kudo, T. Sakata, Electrochemical reduction of high pressure CO2 at pb, hg and in electrodes in an aqueous KHCO3 solution, J. Electroanal. Chem. 394 (1995) 199–203, https://doi.org/10.1016/0022-0728(95)04010-L.
[31] K. Hara, A. Kudo, T. Sakata, Electrochemical reduction of carbon dioxide under high pressure on various electrodes in an aqueous electrolyte, J. Electroanal. Chem. 391 (1995) 141–147, https://doi.org/10.1016/0022-0728(95)03935-A.
[32] K. Hara, A. Tsuneto, A. Kudo, T. Sakata, Electrochemical reduction of CO 2 on a cu electrode under high pressure: factors that determine the product selectivity, J. Electrochem. Soc. 141 (1994) 2097–2103, https://doi.org/10.1149/1.2055067.
[33] J. Li, Y. Kuang, Y. Meng, X. Tian, W.H. Hung, X. Zhang, A. Li, M. Xu, W. Zhou, C. S. Ku, C.Y. Chiang, G. Zhu, J. Guo, X. Sun, H. Dai, Electroreduction of CO2to formate on a copper-based electrocatalyst at high pressures with high energy conversion efficiency, J. Am. Chem. Soc. 142 (2020) 7276–7282, https://doi.org/10.1021/jacs.0c00122.
[34] L. Huang, G. Gao, C. Yang, X.-Y. Li, R.K. Miao, Y. Xue, K. Xie, P. Ou, C.T. Yavuz, Y. Han, G. Magnotti, D. Sinton, E.H. Sargent, X. Lu, Pressure dependence in aqueous-based electrochemical CO2 reduction, Nature Communications 2023 14:1 14 (2023) 1–11. https://doi.org/10.1038/s41467-023-38775-0.
[35] F. Proietto, A. Galia, O. Scialdone, Towards the electrochemical conversion of CO2 to formic acid at an applicative scale: technical and economic analysis of Most promising routes, ChemElectroChem 8 (2021) 2169–2179, https://doi.org/10.1002/celc.202100213.
[36] S. Sabatino, A. Galia, G. Saracco, O. Scialdone, Development of an electrochemical process for the simultaneous treatment of wastewater and the conversion of Carbon dioxide to higher value products, ChemElectroChem 4 (2017) 150–159, https://doi.org/10.1002/CELC.201600475.
[37] K. Yang, R. Kas, W.A. Smith, In Situ Infrared Spectroscopy Reveals Persistent Alkalinity near Electrode Surfaces during CO 2 Electroreduction, (2019). https://doi.org/10.1021/jacs.9b07000.
[38] F. Urbain, P. Tang, N.M. Carretero, T. Andreu, J. Arbiol, J.R. Morante, Tailoring copper foam with silver dendrite catalysts for highly selective Carbon dioxide conversion into Carbon monoxide, ACS Appl. Mater. Interfaces 10 (2018) 43650–43660, https://doi.org/10.1021/ACSAMI.8B15379/ASSET/IMAGES/LARGE/AM-2018-15379V_0004.JPEG.
[39] Q. Zhang, Q. Luo, Z. Qin, L. Liu, Z. Wu, B. Shen, W. Hu, Self-assembly of graphene-encapsulated cu composites for nonenzymatic glucose sensing, ACS Omega 3 (2018) 3420–3428, https://doi.org/10.1021/ACSOMEGA.7B01197/ASSET/IMAGES/LARGE/AO-2017-01197B_0007.JPEG.
[40] D.W. DeWulf, T. Jin, A.J. Bard, Electrochemical and Surface studies of Carbon dioxide reduction to methane and ethylene at copper electrodes in aqueous solutions, J. Electrochem. Soc. 136 (1989) 1686–1691, https://doi.org/10.1149/1.2096993/XML.
[41] K. Xiang, F. Zhu, Y. Liu, Y. Pan, X. Wang, X. Yan, H. Liu, A strategy to eliminate carbon deposition on a copper electrode in order to enhance its stability in CO 2 RR catalysis by introducing crystal defects, Electrochem. Commun. 102 (2019) 72–77, https://doi.org/10.1016/j.elecom.2019.04.001.
[42] Y. Hori, Electrochemical CO2 reduction on metal electrodes, Modern Aspects of Electrochemistry (2008) 89–189, https://doi.org/10.1007/978-0-387-49489-0_3.
[43] C.W. Li, M.W. Kanan, CO 2 reduction at low overpotential on cu electrodes resulting from the reduction of thick cu 2O films, J. Am. Chem. Soc. 134 (2012) 7231–7234, https://doi.org/10.1021/JA3010978/SUPPL_FILE/JA3010978_SI_001.PDF.
[44] M. Aresta, A. Angelini, The carbon dioxide molecule and the effects of its interaction with electrophiles and nucleophiles, Carbon Dioxide and Organometallics 53 (2015) 1–38, https://doi.org/10.1007/3418_2015_93/SCHEMES/4.
[45] D.H. Gibson, Carbon dioxide coordination chemistry: metal complexes and surface-bound species. what relationships? Coord. Chem. Rev. 185–186 (1999) 335–355, https://doi.org/10.1016/S0010-8545(99)00021-1.
[46] I.V. Chernyshova, P. Somasundaran, S. Ponnurangam, On the origin of the elusive first intermediate of CO2 electroreduction, PNAS 115 (2018) E9261–E9270, https://doi.org/10.1073/PNAS.1802256115/SUPPL_FILE/PNAS.1802256115.SAPP.PDF.
[47] R. García-Muelas, F. Dattila, T. Shinagawa, A.J. Martín, J. Pérez-Ramírez, N. López, Origin of the selective electroreduction of Carbon dioxide to formate by chalcogen modified copper, J. Phys. Chem. Lett. 9 (2018) 7153–7159, https://doi.org/10.1021/ACS.JPCLETT.8B03212/ASSET/IMAGES/LARGE/JZ-2018-03212U_0003.JPEG.
[48] S. Sen, D. Liu, G.T.R. Palmore, Electrochemical reduction of CO2 at copper nanofoams, ACS Catal. 4 (2014) 3091–3095, https://doi.org/10.1021/cs500522g.
[49] A.R.T. Morrison, M. Ramdin, L.J.P. Van Der Broeke, W. De Jong, T.J.H. Vlugt, R. Kortlever, Surface coverage as an important Parameter for predicting selectivity trends in electrochemical CO2Reduction, J. Phys. Chem. C 126 (2022) 11927–11936, https://doi.org/10.1021/ACS.JPCC.2C00520/ASSET/IMAGES/LARGE/JP2C00520_0005.JPEG.
[50] J. Hou, X. Chang, J. Li, B. Xu, Q. Lu, Correlating CO coverage and CO electroreduction on cu via high-pressure in situ spectroscopic and reactivity investigations, J. Am. Chem. Soc. 144 (2022) 22202–22211, https://doi.org/10.1021/jacs.2c09956.
[51] D.J. Su, S.Q. Xiang, S.T. Gao, Y. Jiang, X. Liu, W. Zhang, L. Bin Zhao, Z.Q. Tian, Kinetic understanding of catalytic selectivity and product distribution of electrochemical Carbon dioxide reduction reaction, JACS Au (2023), https://doi.org/10.1021/JACSAU.3C00002/ASSET/IMAGES/LARGE/AU3C00002_0009.JPEG.
[52] J.P.-R. and N.L. Sergio Pablo-García, Florentine L. P. Veenstra, Louisa Rui Lin Ting, Rodrigo García-Muelas, Federico Dattila Antonio J. Martín, b Boon Siang Yeo, Mechanistic routes toward C3 products in copper- catalysed CO2 electroreduction, (2022). https://doi.org/10.1039/d1cy01423d.
[53] K. Qi, Y. Zhang, N. Onofrio, E. Petit, X. Cui, J. Ma, J. Fan, H. Wu, W. Wang, J. Li, J. Liu, Y. Zhang, Y. Wang, G. Jia, J. Wu, L. Lajaunie, C. Salameh, D. Voiry, Unlocking direct CO2 electrolysis to C3 products via electrolyte supersaturation, Nat. Catal. (2023), https://doi.org/10.1038/s41929-023-00938-z.

[54] M.C.O. Monteiro, F. Dattila, B. Hagedoorn, R. García-Muelas, N. López, M.T.M. Koper, Absence of CO2 electroreduction on copper, gold and silver electrodes without metal cations in solution, Nature Catalysis 2021 4:8 4 (2021) 654–662. https://doi.org/10.1038/s41929-021-00655-5.
[55] M.R. Singh, Y. Kwon, Y. Lum, J.W. Ager, A.T. Bell, Hydrolysis of electrolyte cations enhances the electrochemical reduction of CO2 over ag and cu, J. Am. Chem. Soc. 138 (2016) 13006–13012, https://doi.org/10.1021/jacs.6b07612.
[56] S. Ringe, E.L. Clark, J. Resasco, A. Walton, B. Seger, A.T. Bell, K. Chan, Understanding cation effects in electrochemical CO2 reduction, energy, Environ. Sci. 12 (2019) 3001–3014, https://doi.org/10.1039/C9EE01341E.
[57] J. Gu, S. Liu, W. Ni, W. Ren, S. Haussener, X. Hu, Modulating electric field distribution by alkali cations for CO2 electroreduction in strongly acidic medium, Nature Catalysis 2022 5:4 5 (2022) 268–276. https://doi.org/10.1038/S41929-022-00761-Y.
[58] J. Resasco, L.D. Chen, E. Clark, C. Tsai, C. Hahn, T.F. Jaramillo, K. Chan, A.T. Bell, Promoter effects of alkali metal cations on the electrochemical reduction of Carbon dioxide, J. Am. Chem. Soc. 139 (2017) 11277–11287, https://doi.org/10.1021/JACS.7B06765/SUPPL_FILE/JA7B06765_SI_001.PDF.
[59] J. Li, X. Li, C.M. Gunathunge, M.M. Waegele, Hydrogen bonding steers the product selectivity of electrocatalytic CO reduction, PNAS 116 (2019) 9220–9229, https://doi.org/10.1073/PNAS.1900761116/SUPPL_FILE/PNAS.1900761116.SAPP.PDF.
[60] H. Zhong, K. Fujii, Y. Nakano, Effect of KHCO 3 concentration on electrochemical reduction of CO 2 on copper electrode, J. Electrochem. Soc. 164 (2017) F923–F927, https://doi.org/10.1149/2.0601709JES/XML.
[61] X. Lv, Z. Liu, C. Yang, Y. Ji, G. Zheng, Tuning structures and microenvironments of cu-based catalysts for sustainable CO2 and CO electroreduction, Acc Mater Res (2022), https://doi.org/10.1021/accountsmr.2c00216.